

## **Classifying seabed sediment type using simulated tidal-induced bed shear stress**

Ward, S.L.; Neill, S.P.; Van Landeghem, K.J.; Scourse, J.D.

### **Marine Geology**

DOI:

[10.1016/j.margeo.2015.05.010](https://doi.org/10.1016/j.margeo.2015.05.010)

Published: 30/05/2015

Publisher's PDF, also known as Version of record

[Cyswllt i'r cyhoeddiad / Link to publication](#)

*Dyfyniad o'r fersiwn a gyhoeddwyd / Citation for published version (APA):*

Ward, S. L., Neill, S. P., Van Landeghem, K. J., & Scourse, J. D. (2015). Classifying seabed sediment type using simulated tidal-induced bed shear stress. *Marine Geology*, 367, 94-104. <https://doi.org/10.1016/j.margeo.2015.05.010>

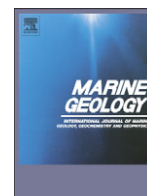
#### **Hawliau Cyffredinol / General rights**

Copyright and moral rights for the publications made accessible in the public portal are retained by the authors and/or other copyright owners and it is a condition of accessing publications that users recognise and abide by the legal requirements associated with these rights.

- Users may download and print one copy of any publication from the public portal for the purpose of private study or research.
- You may not further distribute the material or use it for any profit-making activity or commercial gain
- You may freely distribute the URL identifying the publication in the public portal ?

#### **Take down policy**

If you believe that this document breaches copyright please contact us providing details, and we will remove access to the work immediately and investigate your claim.



# Classifying seabed sediment type using simulated tidal-induced bed shear stress



Sophie L. Ward <sup>\*</sup>, Simon P. Neill, Katrien J.J. Van Landeghem, James D. Scourse

School of Ocean Sciences, Bangor University, Menai Bridge, Isle of Anglesey LL59 5AB, UK

## ARTICLE INFO

### Article history:

Received 19 November 2014

Received in revised form 22 May 2015

Accepted 26 May 2015

Available online 30 May 2015

### Keywords:

Seabed sediments

Sediment transport

Tidal modelling

Bed shear stress

ROMS

Irish Sea

## ABSTRACT

An ability to estimate the large-scale spatial variability of seabed sediment type in the absence of extensive observational data is valuable for many applications. In some physical (e.g., morphodynamic) models, knowledge of seabed sediment type is important for inputting spatially-varying bed roughness, and in biological studies, an ability to estimate the distribution of seabed sediment benefits habitat mapping (e.g., scallop dredging). Although shelf sea sediment motion is complex, driven by a combination of tidal currents, waves, and wind-driven currents, in many tidally energetic seas, such as the Irish Sea, long-term seabed sediment transport is dominated by tidal currents. We compare observations of seabed sediment grain size from 242 Irish Sea seabed samples with simulated tidal-induced bed shear stress from a three-dimensional tidal model (ROMS) to quantitatively define the relationship between observed grain size and simulated bed shear stress. With focus on the median grain size of well-sorted seabed sediment samples, we present predictive maps of the distribution of seabed sediment classes in the Irish Sea, ranging from mud to gravel. When compared with the distribution of well-sorted sediment classifications (mud, sand and gravel) from the British Geological Survey digital seabed sediment map of Irish Sea sediments (DigSBS250), this 'grain size tidal current proxy' (GSTCP) correctly estimates the observed seabed sediment classification in over 73% of the area.

© 2015 The Authors. Published by Elsevier B.V. This is an open access article under the CC BY license (<http://creativecommons.org/licenses/by/4.0/>).

## 1. Introduction

The large-scale redistribution of sediments in shelf sea regions by hydrodynamical processes has direct implications for geological basin and coastal evolution. Seabed sediments also determine the turbidity of water, provide a substrate for marine benthic organisms, host organic matter and are involved in biogeochemical exchanges. Shelf sea sediment motion under the influence of tides, waves and wind-driven currents is a complex phenomenon, the relative contributions of which can change on complex spatial and temporal scales (van der Molen, 2002; Porter-Smith et al., 2004; Neill et al., 2010).

In a tide-dominated shelf sea such as the Irish Sea, sediment transport in the nearshore (coastal) zone can be dominated by wave action, whereas farther offshore the characteristics of seabed sediment distribution are more indicative of the tidal current conditions of a region (e.g., van Dijk and Kleinhans, 2005; Van Landeghem et al., 2009b). A number of studies have used the distribution of peak bed shear stress vectors from tidal models to infer sediment transport pathways and the location of bedload partings around the British Isles (Pingree and Griffiths, 1979; Austin, 1991; Harris and Collins, 1991; Aldridge, 1997; Hall and Davies, 2004; Neill and Scourse, 2009) as well as for the

evolution of bathymetric features such as tidal sand ridges (e.g., Huthnance, 1982; Hulscher et al., 1993), in particular in the Celtic and Irish Seas (e.g., Belderson et al., 1986; Scourse et al., 2009; Van Landeghem et al., 2009a). Pingree and Griffiths (1979) were the first to model the correlation between sand transport paths and the peak bed shear stress vectors caused by the combined  $M_2 + M_4$  tidal currents for many areas on the UK shelf. They found that the direction of bedload transport correlates with the peak bottom bed shear stress vectors ( $M_2 + M_4$ ), and most sand transport occurs in response to the peak current speed over a tidal cycle.

Although the relationship between near-bed hydrodynamics and seabed sediment textures in tidally-dominated areas have been examined (e.g., Uncles, 1983; Knebel and Poppe, 2000; Signell et al., 2000), there remains a need to define and quantify a relationship between a range of simulated current speeds (or bed shear stresses) and a range of seabed sediment types applicable at regional scales. Such a relationship would be valuable for several applications, such as informing expensive field campaigns, or spatial scales for sampling, for incorporating spatially varying drag coefficients into hydrodynamic models, and for habitat mapping (e.g., for scallop dredging) (Robinson et al., 2011).

The aim of this study is to quantify the relationship between simulated (numerically modelled) tidal-induced bed shear stress and observed seabed sediment grain size distribution in the Irish Sea. This relationship is used to develop a proxy, which we refer to hereafter as the 'grain size

<sup>\*</sup> Corresponding author.

E-mail address: [sophie.ward@bangor.ac.uk](mailto:sophie.ward@bangor.ac.uk) (S.L. Ward).

tidal current proxy' (GSTCP), for predicting large-scale distribution in seabed sediment type in the Irish Sea. The study region is introduced in Section 2. In Section 3, the tidal model is described, and the seabed sediment data are presented in Section 3.2, along with a description of the sub-selection of the observational data (Section 3.3). A first-order approximation of the relationship between the simulated bed shear stress and observed seabed sediment grain size is presented in detail in Section 4. The applications and limitations of this proxy are discussed in Section 5.

### 1.1. Sediment transport theory

The effects of currents, waves or by combined current and wave motion on sediment dynamics take place primarily through the friction exerted on the seabed. This frictional force is referred to as the bed shear stress ( $\tau_0$ ) and is expressed as the force exerted by the flow per unit area of bed in terms of the density of water ( $\rho$ ) and the frictional velocity ( $u_*$ ) such that:

$$\tau_0 = \rho u_*^2 \quad (1)$$

Sediment transport (of non-cohesive sediments) occurs when the bed shear stress exceeds the threshold of motion,  $\tau_{cr}$ , or threshold Shields parameter ( $\theta_{cr}$ ) (Shields, 1936), which is a dimensionless form of the bed shear stress and is dependent upon the median grain size,  $d_{50}$ :

$$\theta_{cr} = \frac{\tau_{cr}}{g(\rho_s - \rho)d_{50}} \quad (2)$$

where  $g$  is the gravitational acceleration and  $\rho_s$  is the grain density. The threshold Shields parameter can be plotted against the dimensionless grain size,  $D_*$ , to produce the well-known Shields curve (Shields, 1936), which describes the threshold of motion beneath waves and/or currents. The dimensionless grain size is given by:

$$D_* = \left[ \frac{g(s-1)^{1/3}}{\nu^2} \right] d_{50} \quad (3)$$

where  $\nu$  is the kinematic viscosity of water and  $s$  is the ratio of grain to water density.

Sediment transport occurs through bedload and suspended load transport, and varies depending on the forcing mechanism e.g., whether it is wave-, current- or wind-induced motion, or a combination of mechanisms inducing the motion. Numerous empirically-derived sediment transport formulae are available for total-load sediment transport by currents (e.g., Engelund and Hansen, 1972; van Rijn, 1984a,b,c), waves (e.g., Bailard, 1981) and combined currents and waves (e.g., Bailard, 1981; Soulsby, 1997) in the marine environment. However, these equations have inherent limitations, such as restrictions on applicable water depths, or ranges of grain sizes, and as such are inappropriate for application to regional scales, such as the Irish Sea. Many numerical modelling studies (e.g., Pingree and Griffiths, 1979; Harris and Collins, 1991; Aldridge, 1997; van der Molen, 2002; van der Molen et al., 2004; Griffin et al., 2008; Warner et al., 2008b, 2010) and combined modelling and observational studies (e.g., Harris and Wiberg, 1997; Wiberg et al., 2002) have been conducted in attempts to understand the role of tides and waves on sediment transport in coastal regions. This is the first study aimed at generating maps of estimated sediment grain size distribution on regional scales using both observations and numerical modelling techniques.

## 2. Case study: Irish Sea

It has long been realised that higher-than-average intensity of energy dissipation occurs in the shallow shelf seas around the UK (Flather,

1976; Simpson and Bowers, 1981), with approximately 5 to 6% of the total global tidal dissipation occurring in the Northwest European shelf seas, making it the second most energetic shelf in the world, second only to Hudson Bay (Egbert and Ray, 2001; Egbert, 2004). The Irish Sea (Fig. 1), positioned centrally within the Northwest European shelf seas, is a semi-enclosed body of water, with water depths generally <150 m, and with a north–south trending 250 m deep channel to the northwest of the Isle of Man, between Scotland and Ireland. The tides in the Irish Sea are semi-diurnal (Pingree and Griffiths, 1978), and are dominated by the  $M_2$  and  $S_2$  tidal constituents. Some of the tidal wave, which propagates from the North Atlantic onto the Northwest European shelf, enters the North Sea (from the north) and through the English Channel from the southwest, while some energy passes into the Irish Sea, most of which propagates south to north (Pugh, 1987). The tidal range in the Severn Estuary (in the Bristol Channel) reaches a maximum of ~12 m, the second largest in the world after the Bay of Fundy.

The tidally-dominated Irish Sea is an ideal case study for comparison of observed grain sizes and simulated bed shear stresses given the abundance of existing research and information on the composition of the seabed sediment distribution (e.g., Wilson et al., 2001; Holmes and Tappin, 2005; Blyth-Skyrme et al., 2008; Robinson et al., 2009; Van Landeghem et al., 2009a), as well as extensive surveys by the British Geological Survey (BGS). Irish Sea sediments represent redistributed glacial (or glaciofluvial) materials characterised by a wide range of grain sizes which have the potential to be fractionated by bed shear stress. There is a significant diversity of seabed sediment classifications within the Irish Sea (Fig. 2), including areas of exposed bedrock (mostly limited to the northwest of Anglesey) and patches of semi-consolidated Pleistocene deposits, both covered in places only by thin transient patches of unconsolidated sediment. The majority of the seabed consists

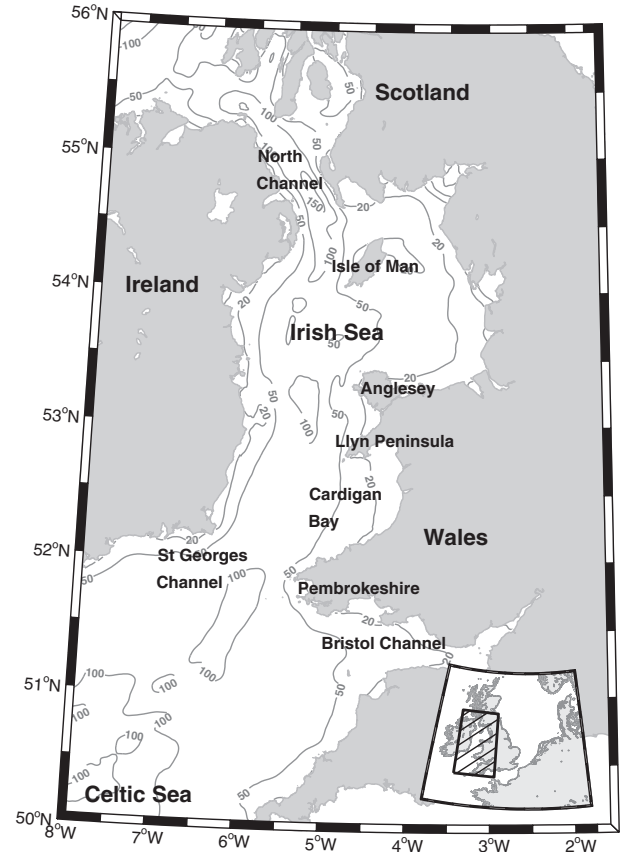
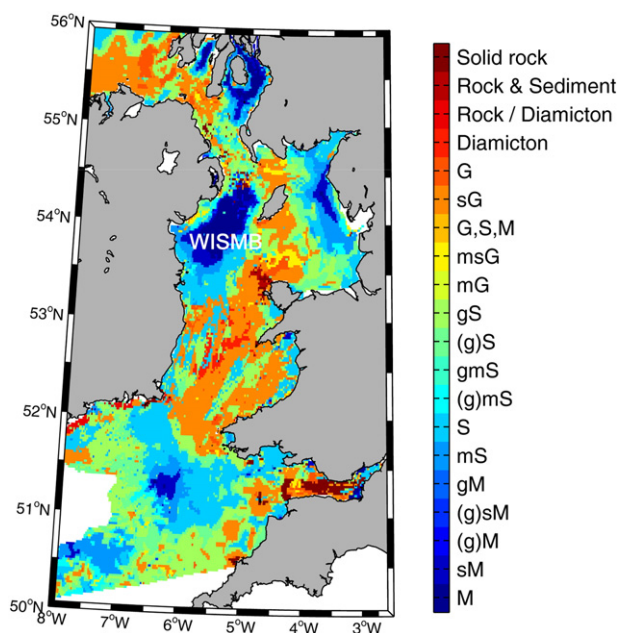


Fig. 1. Bathymetry of the Irish Sea, with water depth (mean sea level) contours in metres. Insert map: the position of the Irish Sea on the Northwest European Shelf.



**Fig. 2.** Digital map of the seabed sediment of the UK waters in the Irish Sea, taken from DigSBS250, using the 20 sediment categories defined by Folk (1954). Grey areas are land and white areas indicate where data are not available. The Western Irish Sea Mud Belt (WISMB) has been labelled.

Digital map reproduced with permission of British Geological Survey © NERC. All rights reserved.

of sands and gravels, consisting of largely reworked glacial sediments. In the southern Irish Sea, sandy gravel is the predominant sediment type. Coarse sediments of glacial and glaciofluvial origin occupy both Cardigan Bay and St George's Channel. In St George's Channel there are several areas of exposed till, covered only by thin transitory sediment. Along the coast of Cardigan Bay is a belt of (mainly) sand which is increasingly muddy towards the mouths of rivers. In the northern Irish Sea there is a band of gravelly sediment, lying to the south and north of the Isle of Man which separates areas of muddy and sandy sediments to the east and west. West of the Isle of Man is a large area of mud, known as the Western Irish Sea Mud Belt, almost entirely surrounded by sandy mud, which itself is surrounded by muddy sand. The muddy sediments in the Irish Sea are largely confined to the Western Irish Sea Mud Belt to the east of the Isle of Man, and to the Celtic Deep (in the central Celtic Sea) (e.g., Jackson et al., 1995).

The UK seabed sediments have been mapped and made available by the BGS as a 1:250,000 scale (~1.1 km grid spacing) digital map product called DigSBS250, and this map product includes most of the Irish Sea (Fig. 2). The map is based on an extensive seabed sample database from grabs of the top 0.1 m, combined with core and dredge samples. For sediment classification, the standard Folk triangle was used, based on the percentage gravel and the sand:mud ratio (Folk, 1954). In the Irish Sea, sediment distribution by classification is typically patchy, with isolated areas of one sediment type (ranging in size from a few metres to many kilometres) surrounded by another sediment type in some places, and with irregular boundaries between categories.

### 3. Methods

#### 3.1. Tidal model

Tidal currents in the Irish Sea were simulated using the three-dimensional Regional Ocean Modeling System (ROMS) (Shchepetkin and McWilliams, 2005), an open-source, free-surface, terrain-following, primitive equations model. The finite-difference approximations of the Reynolds-averaged Navier–Stokes equations are implemented using

the hydrostatic and Boussinesq assumptions. The numerical algorithms of ROMS are described in Shchepetkin and McWilliams (2005).

The domain extent for the Irish Sea tidal model was 8°W to 2.7°W and 50°N to 56°N at a resolution of approximately 1/60° longitude and with variable latitudinal resolution (1/96°–1/105°, i.e., ~1.1 km grid spacing), using a horizontal curvilinear grid. The bathymetry was derived from 30 arcsecond GEBCO (General Bathymetric Chart of the Oceans, ~1 × 1 km resolution), and a minimum water depth of 10 m was applied, which is consistent with other models at this scale and of the region (e.g., Lewis et al., 2014b, 2015). It should be noted that our model application assumes a solid wall along the entire land/sea boundary, and hence alternate wetting and drying of land cells was not included. Given that the model resolution does not fully resolve intertidal regions, the minimum water depth of 10 m, and the lack of wetting and drying, are considered acceptable at this scale.

The model was forced at the boundaries using surface elevation (Chapman boundary conditions) and the  $u$  and  $v$  components of depth-averaged tidal current velocities (Flather boundary conditions), derived from the harmonic constants of the OSU TOPEX/Poseidon Global Inversion Solution 7.2 (TPX07.2, 1/4° resolution globally) (Egbert et al., 1994; Egbert and Erofeeva, 2002). The tidal constituents considered in the derivation of the boundary conditions were  $M_2$  and  $S_2$ . The model was run for 30 days, from which the last 15 days of model output were analysed.

The model was run with analytical expressions for surface momentum stress, bottom and surface salinity fluxes, bottom and surface temperature flux, free-surface boundary conditions, and two-dimensional momentum boundary conditions. The coefficients of vertical harmonic viscosity and diffusion were set to be computed using the generic lengthscale (GLS) turbulence closure scheme model tuned to  $K - \epsilon$  ( $p = 3$ ,  $m = 1.5$ , and  $n = -1$ ) (Umlauf and Burchard, 2003; Warner et al., 2005; Hashemi and Neill, 2014). The tidal model was thus effectively 'three-dimensional barotropic', set to have ten layers in the sigma coordinate, using the coordinate system of Shchepetkin and McWilliams (2005). As much as was possible without compromising the accuracy of the model, the resolution of the layers was increased towards the bed by adjusting the values of the sigma coordinate bottom/surface control parameters in the model runtime options. The option for quadratic bottom drag scheme was implemented, using a bottom drag coefficient of 0.003. The three-dimensional (i.e., depth-varying) bed shear stress is automatically set to be calculated at the mid-depth of each computational cell, and the model was also set to compute and output depth-averaged bed shear stress (and tidal current speeds). So, for example, the 'near-bed' shear stress was calculated at the mid-depth of the lowest vertical layer, the depth of which varied with water depth.

The simulated  $M_2$  and  $S_2$  tidal constituents separated using harmonic analysis (T\_TIDE Pawlowicz et al., 2002) were compared with harmonic constants from six tide gauges within the UK tide gauge network (National Tidal and Sea Level Facility, 2012) (Table 1, Fig. 3).

**Table 1**

Observed and simulated amplitudes ( $h$ , in metres) and phases ( $g$ , in degrees relative to Greenwich) of the  $M_2$  and  $S_2$  tidal constituents. The numbers indicate the position of the tide gauges in Fig. 3. The Scatter Index is the RMSE normalised by the mean of the data, and given as a percentage.

Tide Gauge	Observed				Modelled			
	$M_2$		$S_2$		$M_2$		$S_2$	
	$h$	$g$	$h$	$g$	$h$	$g$	$h$	$g$
Port Erin (1)	1.83	322	0.56	1	1.54	329	0.46	4
Llandudno (2)	2.69	310	0.87	351	2.47	317	0.83	356
Holyhead (3)	1.81	292	0.59	329	1.66	297	0.58	331
Fishguard (4)	1.35	207	0.53	248	1.36	212	0.55	255
Mumbles (5)	3.12	172	1.12	220	3.03	186	1.06	233
Ilfracombe (6)	3.04	162	1.10	209	3.03	174	1.07	221
Scatter Index (%)					6.9	4	6.3	4



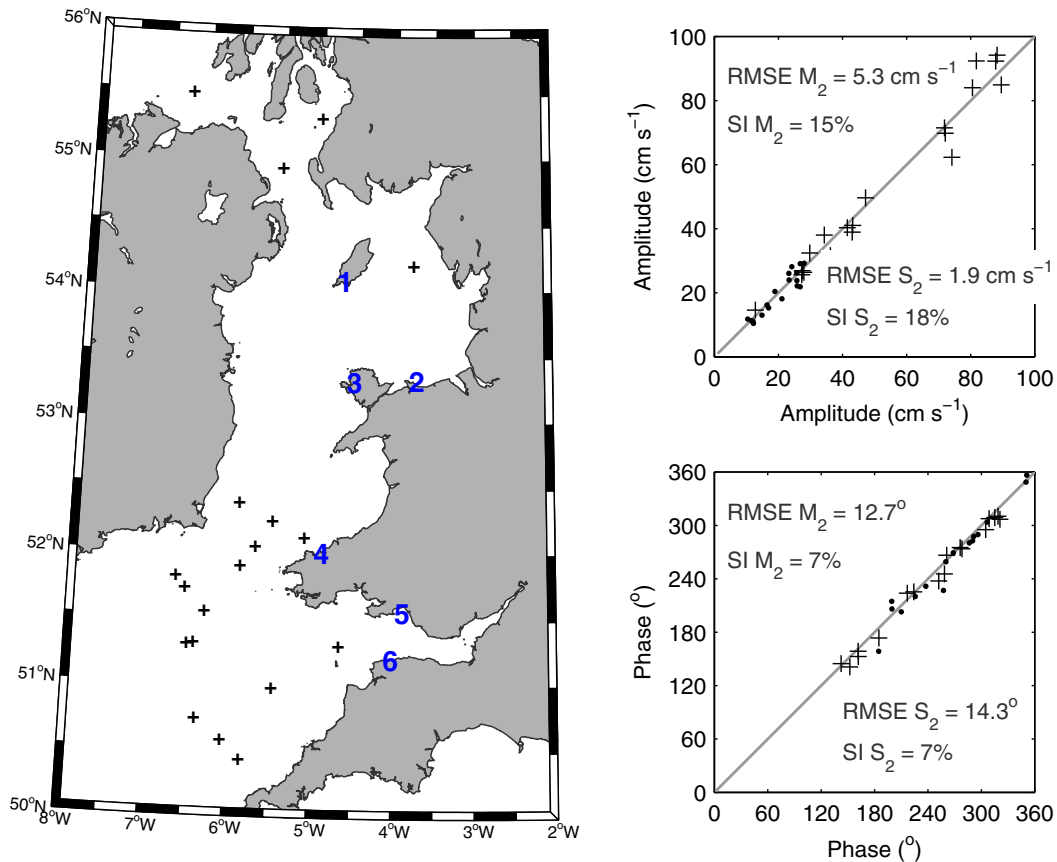


**Fig. 3.** Left panel: the locations of the offshore current meter stations (crosses) and the tide gauge stations (numbers) used in the model validation. Right two panels: comparison between simulated (x-axis) and observed (y-axis) depth-averaged  $M_2$  (crosses) and  $S_2$  (circles) components of tidal current amplitude (upper panel) and phase (lower panel). RMSE = root mean square error, SI = scatter index.

The root mean square error (RMSE) was 16 cm in amplitude and 9° in phase ( $M_2$ ), and 5 cm in amplitude and 8° in phase ( $S_2$ ).

To validate the tidal current speeds (Fig. 3), published current data from 19 offshore current meters within the model domain were used (see Jones, 1983; Davies and Jones, 1990; Young et al., 2000, for further details). The data were compared with the simulated depth-averaged current speed at the grid point nearest the offshore current meter location, which was also analysed using T\_TIDE. The RMSEs of the  $M_2$  tidal currents were 5.3 cm s<sup>-1</sup> in amplitude and 12.7° in phase, and were 1.9 cm s<sup>-1</sup> and 14.3° in phase for the  $S_2$  tidal currents. The scatter index is also provided in Fig. 3, which is the RMSE normalised by the mean of the data, and given as a percentage. The model was found to perform reasonably well when compared with the performance of other models of the region, which were of a similar spatial scale (e.g., Neill et al., 2010; Lewis et al., 2015), giving confidence in the simulated tidal currents.

### 3.2. Seabed sediment data

Data on observed seabed sediments were available from a number of projects, namely HabMap (Robinson et al., 2011), the South West Irish Sea Survey (SWISS, Wilson et al., 2001), the Irish Sea Aggregates Initiative (IMAGIN, Kozachenko et al., 2008), Application of Seabed Acoustic Data in Fish Stocks Assessment and Fishery Performance (ADFISH, Coastal and Marine Research Centre, 2008), and data from the Joint Nature and Conservation Committee (JNCC, e.g., Blyth-Skyrme et al., 2008). Sediment samples from around the Isle of Man were collected and analysed as part of work funded by the Isle of Man, Department of Environment, Food and Agriculture (unpublished data). The full dataset consists of 1105 analysed sediment grab samples, ranging in grain size

from mud to boulders. The samples were analysed using wet sieving and for more detailed analysis of grain size statistics, the results of the wet sieving were analysed using the GRADISTAT software (Blott and Pye, 2001). The granulometric analysis used here for calculating the sample statistics was the graphical method of Folk and Ward (1957).

For comparison with model output, the seabed sediment data were sorted by location and fitted to the computational grid, where each grid cell represented an area of approximately 1.2 km<sup>2</sup>. Samples taken from locations within the same grid cell were combined and the mean, minimum, maximum, and a range of grain size parameters (e.g.,  $d_{50}$ ) were calculated for each grid cell containing data (Fig. 4a). To ensure that no nearshore samples were included, and as an approximation of where nearshore wave effects are likely to dominate sediment transport in this otherwise tidally-dominated region, all samples from locations with water depths ≤ 10 m in the model bathymetry were removed, which was consistent with the minimum water depth set in the model bathymetric grid (Section 3.1). This process of gridding the sediment data, and removing nearshore points resulted in 718 model grid cells containing data (locations shown in Fig. 4a), reduced from the original 1105 samples.

### 3.3. Seabed sediment sorting

Determining which grain size parameter correlated best with simulated bed shear stress was an iterative process. When the median sediment grain size from the 718 gridded sediment samples were compared with simulated peak bed shear stress, there was no discernible correlation (Fig. 4b). Various criteria were thus investigated and applied to the seabed sediment dataset, including grain size limits and degree of sediment sorting. The first grain size parameter to be

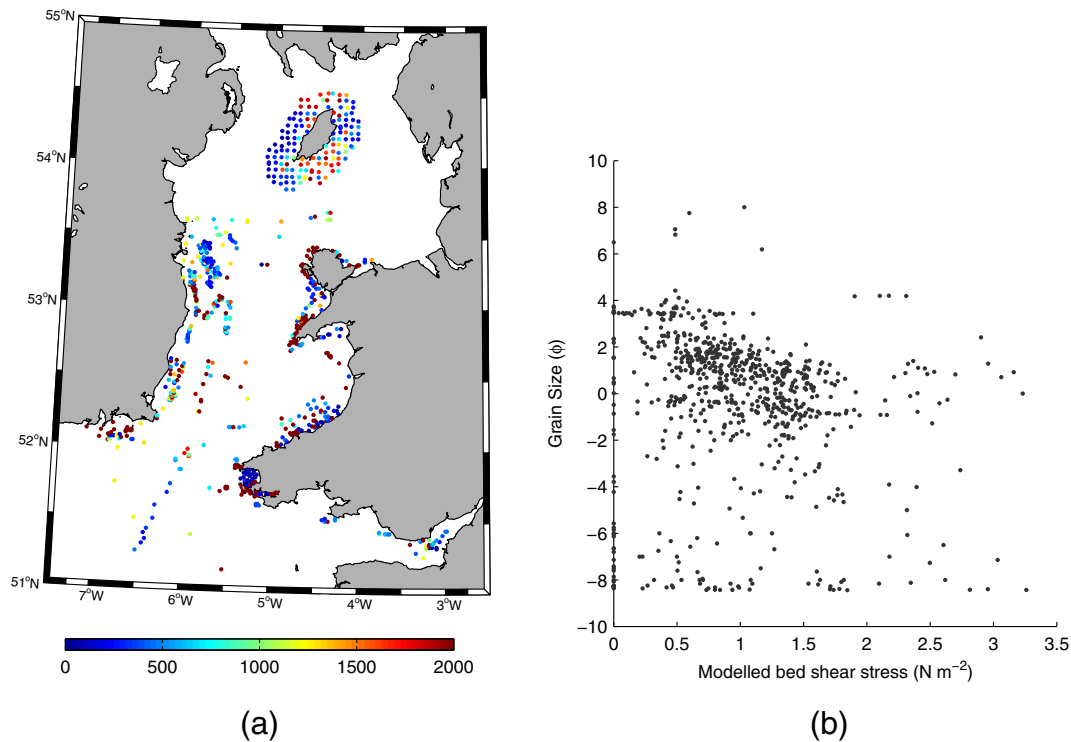


**Fig. 4.** a) Average median grain size,  $d_{50}$  ( $\mu\text{m}$ ), derived from grain size analysis of 1105 seabed sediment samples, which have been combined and gridded into 718 grid cells containing sediment data. b) Correlation between average median grain size,  $d_{50}$  (in  $\phi$  to show the full size range) of all 718 seabed sediment samples and ROMS tidal model output of peak bed shear stress.

considered was sorting, since the accuracy of the calculations of median grain size improved with the degree of sorting of a sample, since it is difficult to calculate a median grain size of a mixed (*poorly-sorted*) sediment sample. Sorting is defined within the GRADISTAT software as the standard deviation (see Blott and Pye, 2001). Furthermore, the GSTCP is based on a relationship between sediment classes that have been reworked by tidal currents, and the factors influencing the spatial distribution of mixed sediment classes is unlikely to be dominated by tidal currents. All *extremely poorly-sorted*, *very poorly-sorted* and *poorly-sorted* samples were thus removed from the seabed sediment dataset. This reduced the sample size considerably, from 718 to 273 samples, consisting of only *moderately-sorted*, *moderately well-sorted*, *well-sorted* and *very well-sorted* samples.

Of the 273 *moderately* to *very well-sorted* samples, 12 had  $d_{50} > 64$  mm (larger than pebbles), and only 8 had  $d_{50} < 4$   $\mu\text{m}$  (very fine silt). These very fine seabed sediment samples were taken off the north coast of the Llŷn Peninsula, and to the northwest of Anglesey. When these very coarse and very fine sediments were considered, there was no clear positive correlation between grain size and simulated bed shear stress. These 20 samples were so few (i.e., <10%) that they were removed from the dataset, hence the remaining 256 seabed sediment samples were all within the sand fraction. The removal of these samples was justified as they did not comprise the mobile fraction, as coarse gravels and cohesive sediments are not representative of the dynamic equilibrium between tidal current speeds and seabed sediment type. Fourteen significant outliers remained, which were fine (or very fine) sands found in areas containing high tidal current speeds (in the Bristol Channel and off the north coast of Pembrokeshire), where simulated peak bed shear stress was  $> 10 \text{ N m}^{-2}$ . These samples were also removed from the seabed sediment dataset as they were likely to be either cohesive or not in dynamic equilibrium, leaving 242 gridded seabed sediment sample points. All of the subset of 242 gridded seabed sediment samples (shown in Fig. 5) were from water depths in the range 10–100 m. Almost half the samples (118 of 242) were from

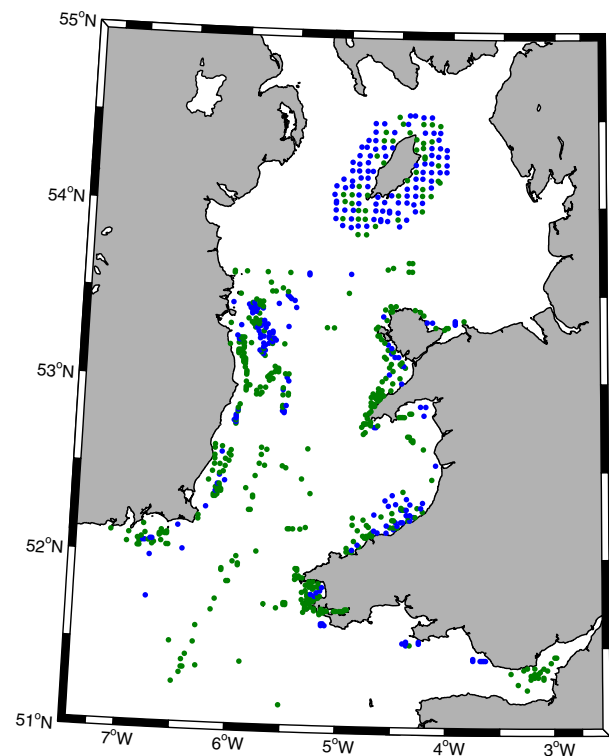


**Fig. 5.** Distribution of gridded seabed sediment samples: blue = 242 samples remaining after application of the various selection criteria, green = 476 samples removed.

water of 10–15 m depth, and 216 (of 242) of the samples were taken in water shallower than 50 m.

## 4. Results

### 4.1. Grain size tidal current proxy (GSTCP)

The spatial variation in the peak tidal-induced bed shear stress across the Irish Sea can be seen in Fig. 6. There are regions of particularly high bed shear stresses in the Bristol Channel (where they exceed  $15 \text{ N m}^{-2}$ ), off the Pembrokeshire coast, northwest of Anglesey, north of the Isle of Man and in the North Channel. Although there is a clearly positive correlation between bed shear stress and seabed sediment grain size (Fig. 7), the relationship is non-linear in nature, as expected from the characteristics of the Shields curve (Shields, 1936) which describes the non-linear variation in the threshold of motion of sediments between currents (and/or waves), or the Hjulström curve (Hjulström, 1935) which describes erosion, deposition or transport of sediment in rivers (i.e., uni-directional flows).

The model outputs of peak bed shear stress were binned into classes of very low through to high bed shear stress: 0–0.5, 0.5–1, 1–1.5, 1.5–2, 2.5–3, 3–4, 4–5, 5–8 and 8–10  $\text{N m}^{-2}$ . The observed  $d_{50}$  from model grid cells with bed shear stress within each class were combined and plotted against the corresponding mid-point of the bed shear stress range

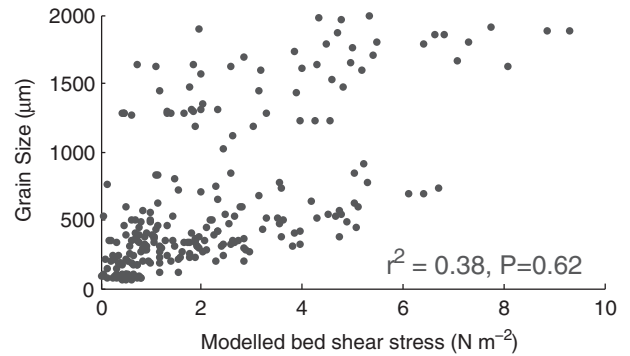


Fig. 7. Correlation between gridded seabed sediment samples (mean  $d_{50}$  in  $\mu\text{m}$ ) and ROMS tidal model output of peak bed shear stress. Samples removed from this dataset included those that were less well sorted than *moderately sorted*, very fine samples ( $<63 \mu\text{m}$ ) in areas of very strong tidal currents, and samples from areas with bed shear stress  $>10 \text{ N m}^{-2}$ .

(Fig. 8a). The minimum and maximum of the gridded  $d_{50}$  were also noted for each of the bed shear stress ranges and are included in Fig. 8a.

A number of sediment classes from the Wentworth scale (Wentworth, 1922) were considered, namely very fine sand (and finer,  $<125 \mu\text{m}$ ), fine sand ( $125\text{--}250 \mu\text{m}$ ), medium sand ( $250\text{--}500 \mu\text{m}$ ), coarse sand ( $500\text{--}1000 \mu\text{m}$ ), very coarse sand ( $1000\text{--}2000 \mu\text{m}$ ) and gravel ( $>2000 \mu\text{m}$ ). The ranges in simulated bed shear stresses from locations in which observations of these sediment classes were made were recorded (Fig. 8b). The values used in the GSTCP are given in Table 2. These seabed sediment size ranges were then applied to the Irish Sea tidal model output of peak bed shear stress, thus demonstrating for the first time a method for predicting large-scale patterns in the distribution of sediment classification for specific simulated bed shear stress values (Fig. 9a). A version of the DigSBS250 map, which only shows selected sediment classes, is provided for comparison (Fig. 9b).

### 4.2. Validating the GSTCP

The main limitation of the validation of the GSTCP is the practical difficulty in acquiring enough seabed sediment grain size data over the shelf. The available grain size data have been used in the development of the proxy, and in the absence of another extensive dataset, an attempt was made at a more ordinal validation of the GSTCP than the qualitative comparison shown in Fig. 9, a significant constraint being the difficulty of estimating a median grain size using Folk sediment classifications. Since samples which were classified as mixed (such as muddy gravel) were eliminated from the sample dataset, a comparison was made between the mapped areas of mud, sand and gravel only from the DigSBS250 (Fig. 10a) with the mud, sand and gravel regions estimated by the proxy. For this comparison the estimated very fine sands (and finer,  $<125 \mu\text{m}$ ) were classified as mud. Fine, medium and coarse sands were simply classified as sands, and estimated grain sizes  $>2000 \mu\text{m}$  were classified as gravel. The spatial differences in observed and estimated areas of mud, sand and gravel are shown in Fig. 10b. The light grey areas in Fig. 10b show areas of the seabed where the estimated and observed seabed sediment classification were in agreement (73% of the non-mixed sediment area). The red and blue patches indicate where the GSTCP underestimated (15%) and overestimated (12%) the observed seabed sediment grain size respectively. It should be noted that the DigSBS250 product is also a generalisation of the Irish Sea seabed sediment types produced from extensive sediment samples (and hence in many areas is also estimated and/or interpolated). The differences in the observed and estimated seabed sediment classification were found to be only between mud and sand, or sand and gravel, and not between gravel and mud. Although tidal asymmetry is not accounted for within the GSTCP, there was no correlation between

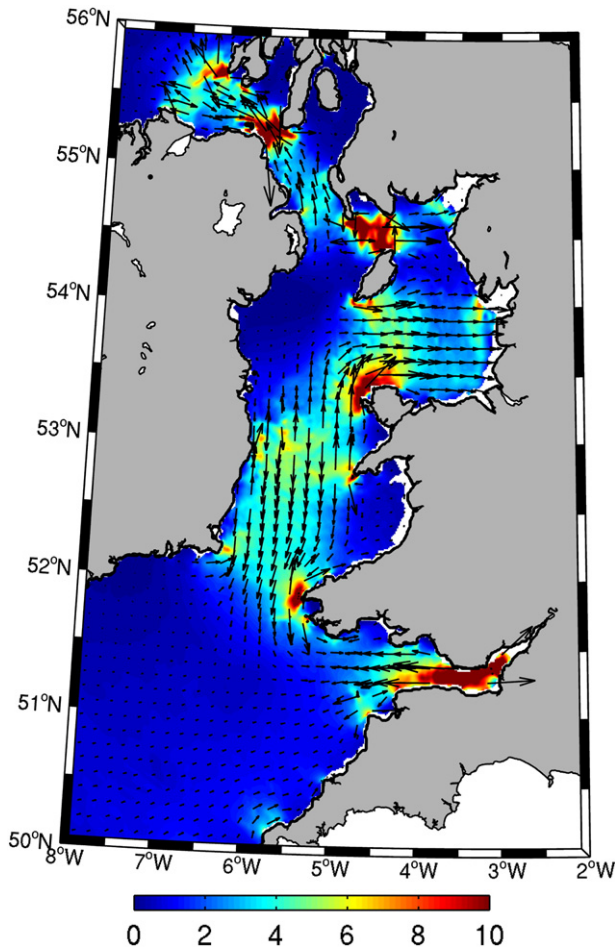
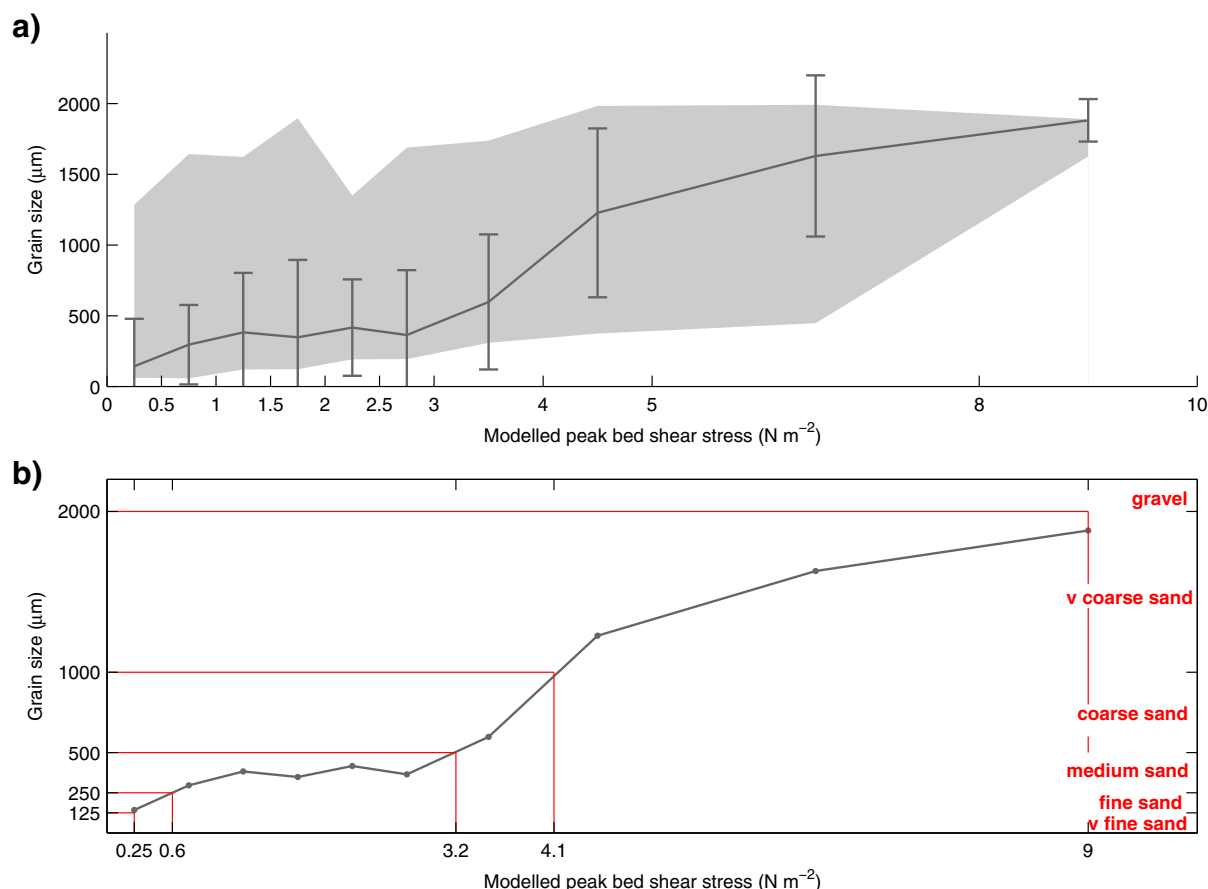


Fig. 6. Simulated 'near-bed' peak ( $M_2 + S_2$ ) tidal-induced bed shear stress in the Irish Sea (in  $\text{N m}^{-2}$ ). Colour scale denotes the bed shear stress magnitude, and vectors denote the direction and magnitude. White areas show additional land mask or where water depths are  $\leq 10 \text{ m}$ .



**Fig. 8.** a) Median  $d_{50}$  and associated standard deviations of gridded seabed sediment samples within specified ranges of simulated bed shear stress (grey line), plotted at the mid-point of the bed shear stress classes (x-axis). The range of gridded  $d_{50}$  are also given (grey fill). b) Median  $d_{50}$  of gridded seabed sediment samples (grey line). The red lines relate to the range of bed shear stress (x-axis) for the different sediment classes (y-axis). The sample sorting and grain size selection criteria were applied to these data.

simulated regions of bed shear stress convergence/divergence and regions of discrepancies between observed and estimated grain sizes.

## 5. Discussion

Predicting (albeit large-scale) patterns in seabed sediment type on regional scales using tidal model output has several key applications, including physical (e.g., morphodynamic) modelling and biological studies, where information regarding the distribution of seabed sediments is important. For example, the GSTCP could be used in ecological studies to identify initial areas of interest based on seabed sediment class, which would then require more focussed investigation (or sampling) of small-scale variations in substrate type. Knowledge of the physical properties of an area, including energy regime, topography and substrate type, is essential for predictive habitat mapping which is used to predict the biological community on the seabed. A tool for predicting large-scale distributions of seabed sediments is very valuable, can reduce the need for expensive field campaigns, or can be

used to identify areas of interest for further work. In addition, the GSTCP can be used to generate predictive maps for seabed sediment evolution over various timescales. Prior to this work there has been no attempt at generating maps of estimated sediment grain size distribution on regional scales. Although this proxy is applicable to high mid-latitude glaciated shelf seas supplied with heterogeneous sediments available for re-distribution post-glacially, the application of this technique of estimating grain size distribution on low-latitude shelf seas may be problematic because of a lack of heterogeneous material available for redistribution.

The GSTCP is essentially an attempt at deriving critical threshold values for sediments in the field which are highly variable in terms of hydrodynamics and sediment dynamics. Although tidal-induced currents dominate sediment transport in much of the Irish Sea, other factors such as waves, the influence of which varies temporally and spatially, play considerable roles in determining sediment dynamics. Rather than there being a definitive threshold condition to define which current speeds displace certain grain sizes, a range of threshold values exist (Paphitis, 2001), due to the complexity and stochastic nature of the factors which can influence sediment transport. This range is not specifically accounted for in the GSTCP, which further highlights the need to consider the GSTCP as a predictor of *large-scale* patterns in seabed sediment type. Defining empirical curves for the threshold of sediment motion (e.g., Hjulstrom, 1935; Shields, 1936; Miller et al., 1977) is notoriously difficult, as there is considerable scatter in the data (Miller et al., 1977; Paphitis, 2001). Although these threshold curves are simple to use, they remain severely restricted by the conditions under which they were developed and, as such, are not applicable to regional model outputs. The fact that selection criteria had to be

**Table 2**  
Details of the grain size tidal current proxy (GSTCP).

Peak simulated bed shear stress range ( $\text{N m}^{-2}$ )	GSTCP grain size range ( $\mu\text{m}$ )	GSTCP sediment classification
<0.25	<125	Very fine sand
.25–0.6	125–250	Fine sand
.6–3.2	250–500	Medium sand
.2–4.1	500–1000	Coarse sand
.1–9	1000–2000	Very coarse sand
>9	>2000	Gravel



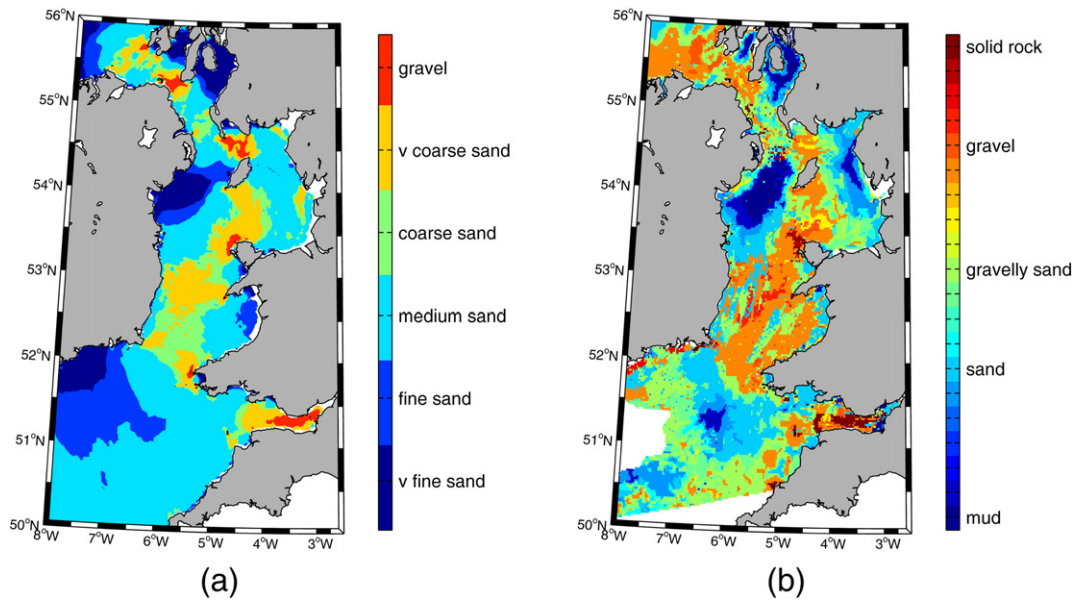


**Fig. 9.** a) Irish Sea seabed sediment distribution estimated by the GSTCP, using simulated bed shear stress. b) Seabed sediments from DigSBS250. Only selected grain size classifications are identified, which indicates a general coarsening of seabed sediment from blue to red on the colour scale.

applied to the seabed sediment dataset in order to produce a discernible trend highlights the limitations of existing theories and empirical equations for estimating sediment transport.

#### 5.1. Discrepancies between observed and estimated seabed sediment grain sizes

The attempt at quantifying the accuracy of the proxy has inherent limitations. For example, the Eastern Irish Sea Mud Belt, east of the

Isle of Man, is comprised of fine mixed sediments (such as sandy mud). These fine mixed sediments are omitted from the comparison and hence the overestimation of the grain size in this area (medium sand) is not highlighted in the proxy validation.

The proxy did not predict some of the observed isolated patches of gravel, such as north of Anglesey, and in the North Channel. The main area where the GSTCP overestimated the sediment classification was in the area of the Western Irish Sea Mud Belt. The area of mud in the western Irish Sea corresponds with low tidal current speeds, suggesting

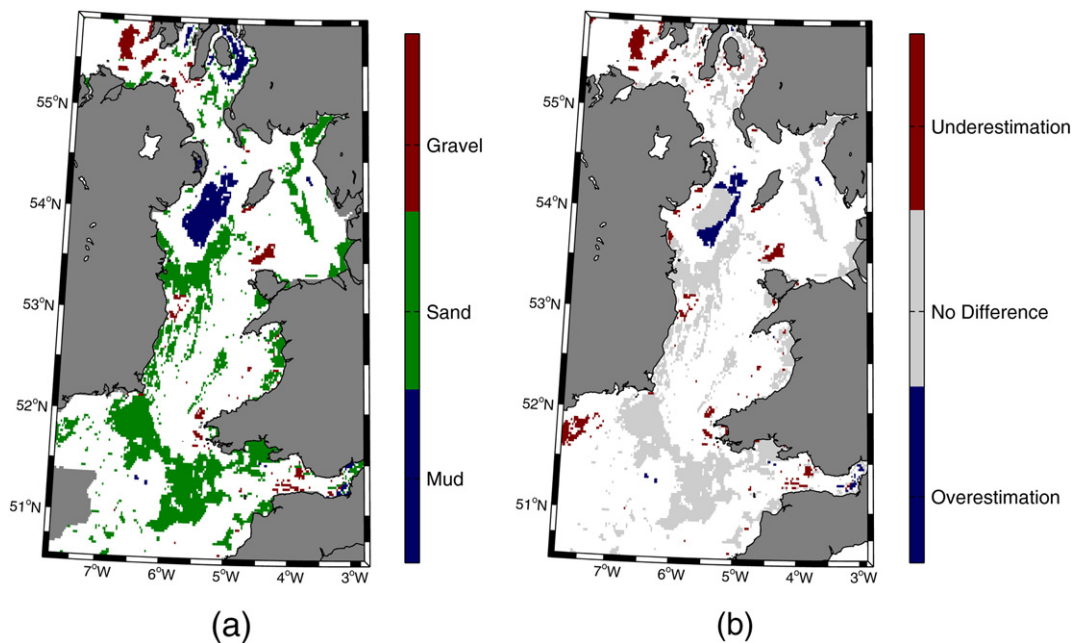


**Fig. 10.** a) Selected seabed sediment classes from DigSBS250 for comparison with the sediment classes estimated by the GSTCP. Only mud (blue), sand (green) and gravel (red) are shown. Mixed sediment classifications are indicated by the white areas. Dark grey areas show land (outlined by the black contour) and where no seabed sediment data were available. b) Difference between the observed and estimated grain size classifications, plotted as the observed minus the estimated. The white areas indicate where seabed sediment was classified as mixed or where there were no seabed sediment data. The light grey areas show areas of agreement between estimated and observed sediment classifications. The red and blue areas indicate where the GSTCP under- and overestimates the seabed sediment grain size respectively.

that this accumulation is strongly controlled by low hydrodynamic energy. However, other factors, such as mixing (by hydrodynamic processes or by bioturbation), likely influence this muddy area, since the upper few metres of seabed sediment appear to date back several thousand years (e.g., [Kershaw, 1986](#)). It is thus not accurate to assume that these sediments have accumulated as a direct result of present-day bed shear stresses only, which could account for the discrepancy between the estimated and observed seabed sediment in this area. There is a narrow band of sandy sediment between the English coast and the Eastern Irish Sea Mud Belt, which has been identified by [Pantin \(1991\)](#) as having formed at a lower sea level, but remains exposed due to wave action, preventing later deposition. The grain size in the area of the mud belt east of the Isle of Man is overestimated by the GSTCP, and is defined as fine sand.

The observed seabed sediment south of Ireland is coarser than the very fine sand (and finer) estimated by the GSTCP, as indicated by the red patch south of Ireland in [Fig. 10b](#), and hence confidence in the results of the GSTCP for this area is low. It is likely that the coarser sediment body in this region is inherited from previous (higher bed shear stress) regimes, and is effectively moribund, since the present-day tidal bed shear stress is too low to entrain the coarse sediments. For example, [Neill et al. \(2010\)](#) found that there was significant enhancement of bed shear stress in the Celtic Sea during deglaciation owing to the magnitude of wave-induced bed shear stress in this region as the shelf was flooded with increasing sea levels. The linear tidal sand ridges of the Celtic Sea are also considered not to be in equilibrium with present-day tidal currents but rather moribund relics of a previously more energetic hydrodynamic regime ([Belderson et al., 1986](#); [Uehara et al., 2006](#); [Scourse et al., 2009](#)). This supports the hypothesis that the coarser sediment distribution in the Celtic Sea is inherited from earlier hydrodynamic regimes. Further, the observed grain sizes north of Ireland (northwest of the North Channel) are coarser than those estimated by the proxy which could be attributable to this region of the shelf being more exposed to wind effects. Where areas of the shelf are exposed to wind (swell) propagating onto the shelf from the Atlantic there is potential for the wave-induced bed shear stress of these longer-period swell waves to penetrate to the seabed ([Neill et al., 2010](#)), thus affecting sediment transport. Cardigan Bay (west coast of mid-Wales) is also dominated by wave action ([Neill et al., 2010](#)) and the GSTCP was found to underestimate the grain size throughout this region.

## 5.2. Limitations of the GSTCP

The GSTCP is developed using only unimodal sediment classes due to the difficulty of calculating a median grain size for mixed sediment classifications. The assumption here is that the distribution of such sediment types will reflect a degree of sorting by tidal currents and hence be indicative of a dynamic equilibrium between tidal-induced bed shear stress and seabed sediment grain size. Consideration of fractional transport of heterogeneous sediments is beyond the scope of this study.

The GSTCP is based on several key assumptions, including assuming tidal current-induced sediment transport only since wave action (which is particularly high during storm events), and wave–current interactions, are not accounted for. Further, other sediment transport mechanisms including fluvial processes, wind drift, storm-surge currents, biological mechanisms, gravitational currents and eddy-diffusive transport of suspended sediment are not considered. Waves can have a significant contribution to sediment dynamics in shelf sea regions (e.g., [van der Molen, 2002](#); [Wiberg et al., 2002](#)) by inducing a stirring mechanism into the hydrodynamic system, thus keeping the sediment suspended and susceptible to net transport by tidal currents. Waves are the primary mechanism for inter-annual variability in sediment transport due to sensitivity to variability in atmospheric (wind) forcing ([Lewis et al., 2014a](#)). In shallower, inshore areas of the Irish Sea, near-shore wave effects become more important than tidal-induced currents

for transporting sediments. The minimum water depth of 10 m used in the simulation was considered appropriate for attempting to omit the influence of such significant nearshore wave action. However, it should be noted that half of the 242 samples on which the GSTCP is based were taken from water depths between 10 and 15 m, and it is likely that waves play a role in the sediment dynamics in such water depths ([van Dijk and Kleinhans, 2005](#)). Since much of the Irish Sea is sheltered by Ireland from the prevailing swell propagating onto the shelf from the North Atlantic, this omission of waters less than 10 m deep is considered reasonable in this first attempt at defining the relationship between simulated tidal-induced bed shear stress and observed seabed sediment grain size.

The Irish Sea is an interesting region in terms of tidal dynamics due to the tides entering this semi-enclosed water body concurrently from the north and the south. The complex features of the overall circulation of the region clearly add complexity to quantifying the relationship between simulated (tidal) bed shear stress and seabed sediment grain sizes. Although the model outputs considered are the peak tidal currents (and hence bed shear stresses) identified during a spring–neap cycle, in reality strong mean currents in varying directions might produce little or zero net sediment transport.

At no point are the sediment sources in the Irish Sea identified or considered, a potential source of error when comparing the output of the GSTCP with the DigSBS250 map. Winnowing and sediment sorting could, for example, leave behind as lag, coarser sediments in tidally quiescent areas and hence the GSTCP would underestimate the grain size in such regions ([Harris and Wiberg, 2002](#)). These samples tend to be poorly-sorted and are likely to be of glacial origin. Consideration of sediment origin, or present-day sources is outside of the scope of this study. Further, the GSTCP does not resolve mixed sediment classifications, or cohesive sediments, which would require alternative sediment transport calculations. The large areas of white (i.e., mixed sediments) in [Fig. 10a](#) highlight the need to conduct research on mixed sediment types, as this omission is a significant limitation.

The tidal model used here assumes a constant drag coefficient (0.003) and does not take into account spatially-varying seabed texture, grain roughness or bedforms (e.g., upstanding rock outcrops in mud belts). In the majority of regional-scale hydrodynamic model studies, spatially-varying bed roughness is not accounted for since extensive observational data regarding seabed sediment type are required for the model set-up. The bottom drag in tidal models is usually described using linear or quadratic friction laws, often using a constant drag coefficient ([Pingree and Griffiths, 1979](#); [van der Molen et al., 2004](#); [Uehara et al., 2006](#); [Neill et al., 2010](#); [Davies et al., 2011](#)). In models which incorporate varying bed roughness, using model output of bed shear stress to estimate seabed sediment type is another iterative problem since varying bottom roughness due to variations in grain size can feed back on tidal energetics, such as bed shear stress and dissipation ([Aldridge and Davies, 1993](#); [Nicolle and Karpytchev, 2007](#); [Kagan et al., 2012](#)). The ability to calculate variable drag coefficients is dependent upon varying the bottom roughness, which is defined as a function of median grain size (e.g., [Li and Amos, 2001](#); [Warner et al., 2005, 2008b](#)). Of more significance, in terms of bed roughness, are larger-scale modulations in bottom roughness such as dunes and ripples ([Van Landeghem et al., 2009a](#); [Kagan et al., 2012](#); [Van Landeghem et al., 2012](#)). In the past, inputting the bottom roughness for calculating varying drag coefficients has been dependent upon observational seabed sediment data (e.g., [Warner et al., 2008a](#); [Wu et al., 2011](#)) or on roughness lengths estimated by model (morphodynamic) subroutines ([Li and Amos, 2001](#)). Further, where comprehensive regional seabed sediment maps exist, it is possible to input variable bed roughness into tidal models (e.g., [Nicolle and Karpytchev, 2007](#)), although in this case the issue of estimating a median grain size of a mixed sediment class remains. This GSTCP addresses the constraints of the above factors by facilitating an estimation of large-scale (spatial) variations in median grain size on a regional scale. Altering bed roughness in tidal models can have

important consequences for flows and associated sediment transport (McCann et al., 2011). For example, increased frictional effects due to increased bed roughness would decrease tidal current velocities and hence affect residual flows. This would have an amplified effect on bed shear stress through the altered drag coefficients and the effect on the current speed.

Despite the limitations of the GSTCP, it is able to define and differentiate between the dominant sediment classifications (mud, sand and gravel) in the Irish Sea. As a first attempt at generating predictive maps of seabed sediment type on a regional scale, the GSTCP is useful for several applications and can be applied until further work which includes coupled tide- and wave modelling, or which incorporates mixed sediment types, becomes available.

### 5.3. Recommendations for improving the GSTCP

A higher resolution tidal model (e.g., <100 m grid spacing) would considerably reduce the need for combining clustered seabed sediment sample data and would better resolve spatial variations in simulated peak bed shear stress. A higher resolution model would also resolve the intertidal regions and so implementation of alternate wetting and drying in the simulations would be important. Coupled tide- and wave modelling (which can be very expensive) would increase the accuracy of the proxy by considering wave-induced sediment transport. In the majority of shelf sea and coastal regions both waves and currents play a role in sediment dynamics; however, their combined effect is not simply a linear addition of the two independent effects (e.g., Soulsby, 1997; van der Molen, 2002; Neill et al., 2010) hence the need for coupled tide- and wave modelling. Furthermore, to resolve the inter-annual variability in the wave climate, multiple years – or even decades – of simulations are required (Neill and Hashemi, 2013) which is also very expensive.

The GSTCP could be further improved by having more observed seabed sediment data with better spatial coverage throughout the Irish Sea and from a greater range of water depths since almost 90% of the samples were taken in water <50 m deep. The most extensive dataset on Irish Sea seabed sediment types has been compiled by the BGS and the data collection spanned several decades. The dataset has been used to generate the digital map product used here (DigSBS250) for comparison with the GSTCP estimations. However, it lacks quantitative data on sediment grain sizes; rather it focusses on sediment classes. The BGS data are therefore unsuitable for the development of the GSTCP but are an invaluable resource in validating the accuracy of the sediment distribution estimated by the GSTCP. The seabed sediment samples used here were readily available and use of many more samples, with better spatial coverage, would require extensive, expensive, further sampling campaigns and data analysis. As highlighted by the need to eliminate mixed sediments from this seabed sediment dataset, quantifying the relationship between currents and mixed sediment grain sizes is a considerable problem that requires extensive further work.

## 6. Conclusions

The proxy for seabed sediment grain size developed here is a first-order approximation, based on the model output of bed shear stress, using a ~1.1 km model grid resolution and six (reasonably well-sorted) sediment classes. The proxy (GSTCP) was successful in estimating 73% of the *well-sorted* sediments and in identifying the main areas of coarse sediments in regions of stronger peak tidal current speeds (and hence high bed shear stress). Discrepancies between maps of observed and estimated grain sizes in the Irish Sea are mainly attributed to a lack of consideration of sediment origin or to wave-induced sediment transport. Despite the limitations of this proxy, the ability to estimate the grain size distribution of seabed sediments on shelf seas such as the Northwest European shelf seas has significant implications for a wide range of applications. Future work should include more seabed

sediment grain size samples, with better coverage across the Irish Sea, and the focus should be on coupled tide- and wave modelling. The proxy could be applied to simulated bed shear stresses from other tidally-energetic shelf sea regions and it would be beneficial to develop proxies for shelf seas with contrasting hydrodynamic regimes. Furthermore, quantification of the relationship between observed seabed sediment grain size of heterogeneous sediment samples and simulated bed shear stresses over regional scales would significantly enhance future similar proxies.

## Acknowledgements

Funding was provided by the Natural Environment Research Council (NERC) through grant NE/I527853/1 (Ph.D. studentship to SLW). The authors are grateful for access to the seabed sediment sample data and would like to acknowledge colleagues collecting and preparing these data through the projects HABMAP, SWISS, IMAGIN, ADFISH, and various projects led by the JNCC, as well as Hilmar Hinz, Lee Murray and Gwladys Lambert for work undertaken on a project funded by the Isle of Man Government (Department of Environment, Food and Agriculture). The author acknowledges modelling support from Patrick Timko and Reza Hashemi. The digital seabed sediment map (DigSBS250) was kindly made available by the BGS. The model simulations were undertaken on High Performance Computing (HPC) Wales, a collaboration between Welsh universities, the Welsh Government and Fujitsu.

## References

- Aldridge, J.N., 1997. Hydrodynamic model predictions of tidal asymmetry and observed sediment transport paths in Morecambe Bay. *Estuar. Coast. Shelf Sci.* 44, 39–56.
- Aldridge, J.N., Davies, A.M., 1993. A high-resolution three-dimensional hydrodynamic tidal model of the Eastern Irish Sea. *J. Phys. Oceanogr.* 23, 207–224. [http://dx.doi.org/10.1175/1520-0485\(1993\)023<0207:AHRTDH>2.0.CO;2](http://dx.doi.org/10.1175/1520-0485(1993)023<0207:AHRTDH>2.0.CO;2).
- Austin, R.M., 1991. Modelling Holocene tides on the NW European continental shelf. *Terra Nova* 3, 276–288.
- Bailard, J.A., 1981. An energetics total load sediment transport model for a plane sloping beach. *J. Geophys. Res.* 86, 10938. <http://dx.doi.org/10.1029/JC086iC11p10938>.
- Belderson, R., Pingree, R., Griffiths, D., 1986. Low sea-level tidal origin of Celtic Sea sand banks – evidence from numerical modelling of M2 tidal streams. *Mar. Geol.* 73, 99–108.
- Blott, S.J., Pye, K., 2001. GRADISTAT: a grain size distribution and statistics package for the analysis of unconsolidated sediments. *Earth Surf. Process. Landf.* 26, 1237–1248.
- Blyth-Skyrme, V., Lindenbaum, C., Verling, E., Van Landeghem, K., Robinson, K., Mackie, A., Darbyshire, T., 2008. Broad-scale biotope mapping of potential reefs in the Irish Sea (north-west of Anglesey). JNCC Report No. 423. Technical Report.
- Coastal and Marine Research Centre, 2008. ADFISH: Application of Seabed Acoustic Data in Fish Stocks Assessment & Fishery Performance URL: <http://www.cmrc.ie/projects/adfish-application-of-seabed-acoustic-data-in-fish-stocks-assessment-fishery-performance.html>.
- Davies, A.M., Jones, J.E., 1990. Application of a three-dimensional turbulence energy model to the determination of tidal currents on the northwest European Shelf. *J. Geophys. Res.* 95, 18143. <http://dx.doi.org/10.1029/JC095iC10p18143>.
- Davies, A.M., Xing, J., Jones, J.E., 2011. A model study of tidal distributions in the Celtic and Irish Sea regions determined with finite volume and finite element models. *Ocean Dyn.* 61, 1645–1667. <http://dx.doi.org/10.1007/s10236-011-0428-1>.
- Egbert, G.D., 2004. Numerical modeling of the global semidiurnal tide in the present day and in the last glacial maximum. *J. Geophys. Res.* 109, C03003. <http://dx.doi.org/10.1029/2003JC001973>.
- Egbert, G.D., Erofeeva, S.Y., 2002. Efficient inverse modeling of barotropic ocean tides. *J. Atmos. Ocean. Technol.* 19, 183–204. [http://dx.doi.org/10.1175/1520-0426\(2002\)019<0183:EIMOBO>2.0.CO;2](http://dx.doi.org/10.1175/1520-0426(2002)019<0183:EIMOBO>2.0.CO;2).
- Egbert, G.D., Ray, R.D., 2001. Estimates of M2 tidal energy dissipation from TOPEX/Poseidon altimeter data. *J. Geophys. Res.* 106, 22475. <http://dx.doi.org/10.1029/2000JC000699>.
- Egbert, G.D., Bennett, A.F., Foreman, M.G.G., 1994. TOPEX/POSEIDON tides estimated using a global inverse model. *J. Geophys. Res.* 99, 24821. <http://dx.doi.org/10.1029/94JC01894>.
- Engelund, F., Hansen, E., 1972. *A Monograph on Sediment Transport in Alluvial Streams*. 3rd edn. Technical Press, Copenhagen (Technical Report).
- Flather, R.A., 1976. A tidal model of the north-west European continental shelf. *Memoires de la Society Royal des Sciences de Liege* 6 series, pp. 141–164.
- Folk, R., 1954. The distinction between grain size and mineral composition in sedimentary rock nomenclature. *J. Geol.* 62, 344–359.
- Folk, R., Ward, W., 1957. Brazos River bar: a study in the significance of grain size parameters. *J. Sediment. Petrol.* 27, 3–26.
- Griffin, J.D., Hemer, M.A., Jones, B.G., 2008. Mobility of sediment grain size distributions on a wave dominated continental shelf, southeastern Australia. *Mar. Geol.* 252, 13–23. <http://dx.doi.org/10.1016/j.margeo.2008.03.005>.



- Hall, P., Davies, A.M., 2004. Modelling tidally induced sediment-transport paths over the northwest European shelf: the influence of sea-level reduction. *Ocean Dyn.* 54, 126–141. <http://dx.doi.org/10.1007/s10236-003-0070-7>.
- Harris, P., Collins, M., 1991. Sand transport in the Bristol Channel: bedload parting zone or mutually evasive transport pathways? *Mar. Geol.* 101, 209–216.
- Harris, C.K., Wiberg, P.L., 1997. Approaches to quantifying long-term continental shelf sediment transport with an example from the Northern California STRESS mid-shelf site. *Cont. Shelf Res.* 17, 1389–1418.
- Harris, C.K., Wiberg, P., 2002. Across-shelf sediment transport: interactions between suspended sediment and bed sediment. *J. Geophys. Res.* 107.
- Hashemi, M.R., Neill, S.P., 2014. The role of tides in shelf-scale simulations of the wave energy resource. *Renew. Energy* 69, 300–310. <http://dx.doi.org/10.1016/j.renene.2014.03.052>.
- Hjulstrom, F., 1935. Study of the morphological activity of rivers as illustrated by the Furis. *Bull. Geol. Inst. Univ. Uppsala* 25, 221–527.
- Holmes, R., Tappin, D., 2005. DTI Strategic Assessment Area 6, Irish Sea, seabed and surficial geology and processes. British Geological Survey Commissioned Report, CR/05/057. Technical Report.
- Hulscher, S.J., de Swart, H.E., de Vriend, H.J., 1993. The generation of offshore tidal sand banks and sand waves. *Cont. Shelf Res.* 13, 1183–1204. [http://dx.doi.org/10.1016/0278-4343\(93\)90048-3](http://dx.doi.org/10.1016/0278-4343(93)90048-3).
- Huthnance, J.M., 1982. On one mechanism forming linear sand banks. *Estuar. Coast. Shelf Sci.* 14, 79–99. [http://dx.doi.org/10.1016/S0302-3524\(82\)80068-6](http://dx.doi.org/10.1016/S0302-3524(82)80068-6).
- Jackson, D.I., Jackson, A.A., Evans, D., Wingfield, R.T.R., Barnes, R.P., Arthur, M.J., 1995. The geology of the Irish Sea. (HMSO). Technical Report.
- Jones, J., 1983. Charts of O1, K1, N2, M2 and S2 Tides in the Celtic Sea including M2 and S2 Tidal Currents. Technical Report.
- Kagan, B.A., Sofina, E.V., Rashidi, E., 2012. The impact of the spatial variability in bottom roughness on tidal dynamics and energetics, a case study: the M2 surface tide in the North European Basin. *Ocean Dyn.* 62, 1425–1442. <http://dx.doi.org/10.1007/s10236-012-0571-3>.
- Kershaw, P., 1986. Radiocarbon dating of Irish Sea sediments. *Estuar. Coast. Shelf Sci.* 23, 295–303. [http://dx.doi.org/10.1016/0272-7714\(86\)90029-6](http://dx.doi.org/10.1016/0272-7714(86)90029-6).
- Knebel, H.J., Poppe, L.J., 2000. Seafloor environments within Long Island Sound: a regional overview. *J. Coast. Res.* 16, 533–550.
- Kozachenko, M., Fletcher, R., Sutton, G., Montey, X., Van Landeghem, K., Wheeler, A., Lassoud, Y., Cooper, A., Nicoll, C., 2008. A geological appraisal of marine aggregate resources in the southern Irish Sea. Technical report produced for the Irish Sea. Technical report produced for the Irish Sea Marine Aggregates Initiative (IMAGIN) project funded under the INTERREG IIA Programme. Technical Report.
- Lewis, M., Neill, S., Elliott, A.J., 2014a. Inter-annual variability of two contrasting offshore sand banks in a region of extreme tidal range. *J. Coast. Res.* 31, 265–275.
- Lewis, M., Neill, S., Hashemi, M., Reza, M., 2014b. Realistic wave conditions and their influence on quantifying the tidal stream energy resource. *Appl. Energy* 136, 495–508. <http://dx.doi.org/10.1016/j.apenergy.2014.09.061>.
- Lewis, M., Neill, S., Robins, P., Hashemi, M., 2015. Resource assessment for future generations of tidal-stream energy arrays. *Energy* 83, 403–415. <http://dx.doi.org/10.1016/j.energy.2015.02.038>.
- Li, M.Z., Amos, C.L., 2001. SEDTRANS96: the upgraded and better calibrated sediment-transport model for continental shelves. *Comput. Geosci.* 27, 619–645. [http://dx.doi.org/10.1016/S0098-3004\(00\)00120-5](http://dx.doi.org/10.1016/S0098-3004(00)00120-5).
- McCann, D.L., Davies, A.G., Bennell, J.D., 2011. Bed roughness feedback in TELEMAC-2D and SISYPHE. Proceedings of the XVIII Telemac and Mascaret User Club, pp. 99–104.
- Miller, M.C., McCave, I.N., Komar, P.D., 1977. Threshold of sediment motion under unidirectional currents. *Sedimentology* 24, 507–527. <http://dx.doi.org/10.1111/j.1365-3091.1977.tb00136.x>.
- National Tidal and Sea Level Facility, 2012. Real-time data – UK National Tide Gauge Network URL: <http://www.ntsfl.org.uk/data/uk-network-real-time>.
- Neill, S.P., Hashemi, M.R., 2013. Wave power variability over the northwest European shelf seas. *Appl. Energy* 106, 31–46. <http://dx.doi.org/10.1016/j.apenergy.2013.01.026>.
- Neill, S.P., Scourse, J.D., 2009. The formation of headland/island sandbanks. *Cont. Shelf Res.* 29, 2167–2177. <http://dx.doi.org/10.1016/j.csr.2009.08.008>.
- Neill, S.P., Scourse, J.D., Uehara, K., 2010. Evolution of bed shear stress distribution over the northwest European shelf seas during the last 12,000 years. *Ocean Dyn.* 60, 1139–1156. <http://dx.doi.org/10.1007/s10236-010-0313-3>.
- Nicoll, A., Karpytchev, M., 2007. Evidence for spatially variable friction from tidal amplification and asymmetry in the Pertuis Breton (France). *Cont. Shelf Res.* 27, 2346–2356. <http://dx.doi.org/10.1016/j.csr.2007.06.005>.
- Pantin, H.M., 1991. Seabed sediments around the United Kingdom: their bathymetric and physical environment, grain size, mineral composition and associated bedforms. Technical Report. British Geological Survey Marine Geology Series research report, SB/90/1.
- Paphitis, D., 2001. Sediment movement under unidirectional flows: an assessment of empirical threshold curves. *Coast. Eng.* 43, 227–245. [http://dx.doi.org/10.1016/S0378-3839\(01\)00015-1](http://dx.doi.org/10.1016/S0378-3839(01)00015-1).
- Pawlowicz, R., Beardsley, B., Lentz, S., 2002. Classical tidal harmonic analysis including error estimates in MATLAB using T\_TIDE. *Comput. Geosci.* 28, 929–937.
- Pingree, R.D., Griffiths, D.K., 1978. Tidal fronts on the shelf seas around the British Isles. *J. Geophys. Res.* 83, 4615–4622. <http://dx.doi.org/10.1029/JC083iC09p04615>.
- Pingree, R.D., Griffiths, D.K., 1979. Sand transport paths around the British Isles resulting from M2 and M4 tidal interactions. *J. Mar. Biol. Assoc. U. K.* 59, 497–513.
- Porter-Smith, R., Harris, P., Andersen, O., Coleman, R., Greenslade, D., Jenkins, C., 2004. Classification of the Australian continental shelf based on predicted sediment threshold exceedance from tidal currents and swell waves. *Mar. Geol.* 211, 1–20. <http://dx.doi.org/10.1016/j.margeo.2004.05.031>.
- Pugh, D.T., 1987. Tides, Surges and Mean Sea-level vol. 5. John Wiley & Sons, Ltd., Chichester. [http://dx.doi.org/10.1016/0264-8172\(88\)90013-X](http://dx.doi.org/10.1016/0264-8172(88)90013-X).
- Robinson, K., Darbyshire, T., Van Landeghem, K., Lindenbaum, C., McBrean, F., Creavan, S., Ramsay, K., Mackie, A., Mitchell, N., Wheeler, A., Wilson, J., O'Beim, F., 2009. Habitat Mapping for Conservation and Management of the Southern Irish Sea (HABMAP) I: seabed surveys. Studies in Marine Biodiversity and Systematics from the National Museum of Wales. Technical Report.
- Robinson, K., Ramsay, K., Lindenbaum, C., Frost, N., Moore, J., Wright, A., Petrey, D., 2011. Predicting the distribution of seabed biotopes in the southern Irish Sea. *Cont. Shelf Res.* 31, S120–S131. <http://dx.doi.org/10.1016/j.csr.2010.01.010>.
- Scourse, J.D., Uehara, K., Wainwright, A., 2009. Celtic Sea linear tidal sand ridges, the Irish Sea Ice Stream and the Fleuve Manche: Palaeotidal modelling of a transitional passive margin depositional system. *Mar. Geol.* 259, 102–111. <http://dx.doi.org/10.1016/j.margeo.2008.12.010>.
- Shchepetkin, A.F., McWilliams, J.C., 2005. The regional oceanic modeling system (ROMS): a split-explicit, free-surface, topography-following-coordinate oceanic model. *Ocean Model.* 9, 347–404. <http://dx.doi.org/10.1016/j.ocemod.2004.08.002>.
- Shields, A., 1936. Application of Similarity Principles and Turbulence Research to Bedload Movement. Technical Report. Hydrodynamics Laboratory, California Institute of Technology.
- Signell, R.P., List, J.H., Farris, A.S., 2000. Bottom currents and sediment transport in Long Island Sound: a modeling study. *J. Coast. Res.* 16, 551–566.
- Simpson, J., Bowers, D., 1981. Models of stratification and frontal movement in shelf seas. *Deep Sea Res. A Oceanogr. Res. Pap.* 28, 727–738.
- Soulsby, R.L., 1997. Dynamics of Marine Sand. Thomas Telford, London.
- Uehara, K., Scourse, J.D., Horsburgh, K.J., Lambeck, K., Purcell, A.P., 2006. Tidal evolution of the northwest European shelf seas from the Last Glacial Maximum to the present. *J. Geophys. Res.* 111, C09025. <http://dx.doi.org/10.1029/2006JC003531>.
- Umlauf, L., Burchard, H., 2003. A generic length-scale equation for geophysical turbulence models. *J. Mar. Res.* 61, 235–265. <http://dx.doi.org/10.1357/00222400322005087>.
- Uncles, R.J., 1983. Modeling tidal stress, circulation, and mixing in the Bristol Channel as a prerequisite for ecosystem studies. *Can. J. Fish. Aquat. Sci.* 40, s8–s19. <http://dx.doi.org/10.1139/f83-265>.
- van der Molen, J., 2002. The influence of tides, wind and waves on the net sand transport in the North Sea. *Cont. Shelf Res.* 22, 2739–2762. [http://dx.doi.org/10.1016/S0278-4343\(02\)00124-3](http://dx.doi.org/10.1016/S0278-4343(02)00124-3).
- van der Molen, J., Gerrits, J., de Swart, H., 2004. Modelling the morphodynamics of a tidal shelf sea. *Cont. Shelf Res.* 24, 483–507. <http://dx.doi.org/10.1016/j.csr.2003.12.001>.
- van Dijk, T.A.G.P., Kleinans, M.G., 2005. Processes controlling the dynamics of compound sand waves in the North Sea, Netherlands. *J. Geophys. Res.* 110, F04S10. <http://dx.doi.org/10.1029/2004JF000173>.
- Van Landeghem, K.J., Uehara, K., Wheeler, A.J., Mitchell, N.C., Scourse, J.D., 2009a. Post-glacial sediment dynamics in the Irish Sea and sediment wave morphology: data-model comparisons. *Cont. Shelf Res.* 29, 1723–1736. <http://dx.doi.org/10.1016/j.csr.2009.05.014>.
- Van Landeghem, K.J., Wheeler, A.J., Mitchell, N.C., Sutton, G., 2009b. Variations in sediment wave dimensions across the tidally dominated Irish Sea, NW Europe. *Mar. Geol.* 263, 108–119. <http://dx.doi.org/10.1016/j.margeo.2009.04.003>.
- Van Landeghem, K.J., Baas, J.H., Mitchell, N.C., Wilcockson, D., Wheeler, A.J., 2012. Reversed sediment wave migration in the Irish Sea, NW Europe: a reappraisal of the validity of geometry-based predictive modelling and assumptions. *Mar. Geol.* 295, 95–112.
- van Rijn, L.C., 1984a. Sediment transport, part I: bed load transport. *J. Hydraul. Eng.* 110, 1431–1456.
- van Rijn, L.C., 1984b. Sediment transport, part II: suspended load transport. *J. Hydraul. Eng.* 110, 1613–1641. [http://dx.doi.org/10.1061/\(ASCE\)0733-9429\(1984\)110:11\(1613\)](http://dx.doi.org/10.1061/(ASCE)0733-9429(1984)110:11(1613)).
- van Rijn, L.C., 1984c. Sediment transport, part III: bed forms and alluvial roughness. *J. Hydraul. Eng.* 110, 1733–1754. [http://dx.doi.org/10.1061/\(ASCE\)0733-9429\(1984\)110:12\(1733\)](http://dx.doi.org/10.1061/(ASCE)0733-9429(1984)110:12(1733)).
- Warner, J.C., Sherwood, C.R., Arango, H.G., Signell, R.P., 2005. Performance of four turbulence closure models implemented using a generic length scale method. *Ocean Model.* 8, 81–113. <http://dx.doi.org/10.1016/j.ocemod.2003.12.003>.
- Warner, J.C., Butman, B., Dalyander, P.S., 2008a. Storm-driven sediment transport in Massachusetts Bay. *Cont. Shelf Res.* 28, 257–282. <http://dx.doi.org/10.1016/j.csr.2007.08.008>.
- Warner, J.C., Sherwood, C.R., Signell, R.P., Harris, C.K., Arango, H.G., 2008b. Development of a three-dimensional, regional, coupled wave, current, and sediment-transport model. *Comput. Geosci.* 34, 1284–1306. <http://dx.doi.org/10.1016/j.cageo.2008.02.012>.
- Warner, J.C., Armstrong, B., He, R., Zambon, J.B., 2010. Development of a Coupled Ocean – Atmosphere – Wave – Sediment Transport (COAWST) modeling system. *Ocean Model.* 35, 230–244. <http://dx.doi.org/10.1016/j.ocemod.2010.07.010>.
- Wentworth, C.K., 1922. A scale of grade and class terms for clastic sediments. *J. Geol.* 30, 377–392.
- Wiberg, P.L., Drake, D.E., Harris, C.K., Noble, M., 2002. Sediment transport on the Palos Verdes shelf over seasonal to decadal time scales. *Cont. Shelf Res.* 22, 987–1004. [http://dx.doi.org/10.1016/S0278-4343\(01\)00116-9](http://dx.doi.org/10.1016/S0278-4343(01)00116-9).
- Wilson, J.G., Mackie, A.S.Y., O'Connor, B.D.S., Rees, E.I.S., Darbyshire, T., 2001. Benthic Biodiversity in the southern Irish Sea 2. The South-West Irish Sea Survey (SWISS). Studies in Marine Biodiversity and Systematics from the National Museum of Wales. BIOMÖR Reports 2(1). Technical Report.
- Wu, Y., Chaffey, J., Greenberg, D.A., Colbo, K., Smith, P.C., 2011. Tidally-induced sediment transport patterns in the upper Bay of Fundy: a numerical study. *Cont. Shelf Res.* 31, 2041–2053. <http://dx.doi.org/10.1016/j.csr.2011.10.009>.
- Young, E.F., Aldridge, J.N., Brown, J., 2000. Development and validation of a three-dimensional curvilinear model for the study of fluxes through the North Channel of the Irish Sea. *Cont. Shelf Res.* 20, 997–1035.